<<Research Paper>> Journal of the Korean Vacuum Society Vol.15 No.5, September 2006, pp.534~540

Sol-gel growth and structural, electrical, and optical properties of vanadium-based oxide thin films

Young Ran Park and Kwang Joo Kim*

Department of Physics, Konkuk University, Seoul 143-701, Korea

(Received July 10, 2006)

Thin films of V_2O_3, VO_2, and V_2O_5 were obtained from a single precursor solution through post-annealing processes under different annealing conditions. As annealed in air, the deposited films became V_2O_5 with orthorhombic crystal structure, while they were V_2O_3 and VO_2 with rhombohedral and monoclinic crystal structure as annealed in vacuums with base pressure of 1×10^{-6} Torr and with 10 mTorr O_2 pressure, respectively. Electrical and optical measurements indicated that the V_2O_5 and VO_2 films are semiconducting, while the V_2O_3 films are metallic at room temperature. Chromium doping in VO_2 resulted in a decrease of the resistivity and changed the conduction type from n-type to p-type. 10% Cr-doped VO_2 films were found to have orthorhombic crystal structure, which is different from that of the undoped VO_2. Spectral features in the optical absorption spectra of all the films were interpreted as the transitions involving O *2p* and V *3d* bands. The crystal-field splittings between t_{2g} and e_g states of the V *3d* bands are estimated to be about 1.5 and 1.0 eV for V_2O_5 and VO_2, respectively.

Keywords : Vanadium oxide, Sol-gel, Structural properties, Optical properties

Ⅰ. Introduction

Recently, vanadium-based oxides have been found to exhibit interesting physical and chemical properties applicable for sensors, catalysts, rechargeable batteries, and magneto-electronic devices etc. As the oxidation state of V ion increases from +3 to +5 in the compound V_xO_y, the electrical properties were found to vary from metallic to insulating at room temperature. V_2O_3 is known to undergo a Mott metal-insulator (MI) transition along with a structural change from rhombohedral to monoclinic as the temperature decreases below 168 K [1]. For VO_2 such MI transition occurs near 341 K along with a tetragonal to monoclinic phase transformation [2,3]. V_2O_5 with the highest oxidation state of V ion is known to maintain structural stability with an orthorhombic structure. However, these oxides have not been well characterized in thin-film form, despite the importance for device applications. Besides V_2O_3, VO_2, and V_2O_5, there are many intermediate phases such as V_3O_5, V_4O_7, V_5O_9, V_6O_{11}, V_7O_{13}, V_6O_{13}, V_4O_9, and V_3O_7. Furthermore, the oxygen stoichiometry can be easily broken and the sample becomes either a form of VO_x or a mixed phase.

In the present work, various vanadium oxide thin films have been prepared by a sol-gel

* [E-mail] kjkim@konkuk.ac.kr

method employing spin-coating. Single-phased V_2O_3, VO_2, and V_2O_5 films could be obtained from a single precursor solution by varying post-annealing condition on the spin-coated film. A phase transformation was observed from monoclinic to orthorhombic structure by Cr doping on VO_2. A decrease of the electrical resistivity as well as change of conduction type from n to p was also observed for the Cr-doped VO_2 films. The optical constants of the vanadium-oxide films were measured by spectroscopic ellipsometry (SE) in the visible-ultraviolet range and the observed absorption structures are interpreted in terms of transitions involving O *2p* and V *3d* states.

Ⅱ. Experimental

The precursor solution for V_2O_3, VO_2, and V_2O_5 thin film fabrication by the present sol-gel method was prepared by dissolving $(C_5H_8O_2)_2VO$ powder into a mixed solution of 2-methoxyethanol and monoethanolamine at 170 °C. For Cr or Fe doping $Cr(NO_3)_3 \cdot 9H_2O$ or $Fe(NO_3)_3 \cdot 9H_2O$ was dissolved together. The solution was spin-coated on $Al_2O_3(0001)$ substrate at 3000 rpm for 20 sec. Then the substrate was heated at 230 °C for 3 min after each deposition. This process was repeated for increasing the film thickness. The thickness of the present films was about 1 μm, estimated by scanning electron microscopy. The deposited films became V_2O_3, VO_2, and V_2O_5 depending on the post-annealing condition such as temperature and O_2-gas partial pressure.

The crystalline structure of the deposited films was investigated by X-ray diffraction (XRD) measurements using Cu Kα radiation. The transport properties of the films were investigated by Hall effect measurements, performed in the van der Pauw configuration under a magnetic field of 0.5 T. Optical constants of the films were measured by SE at room temperature with a rotating-analyzer ellipsometer in the visible-ultraviolet range with the energy interval of 0.02 eV. Ellipsometry measures the amplitude and the phase of the complex reflectance ratio ρ (= r_p/r_s) of the p (parallel) and s (perpendicular) field components of the light beam defined with respect to the plane of incidence of the sample. Then the dielectric function ε (= ε_1 + i ε_2) of the sample is obtained from the equation

$$\varepsilon = \sin^2\phi + \sin^2\phi \tan^2\phi \left(\frac{1-\rho}{1+\rho}\right)^2 \quad (1)$$

by assuming an optically flat boundary between the sample and the air. All the spectra were taken at an angle of incidence (ϕ) of 70° and a fixed polarizer angle of 45° from the plane of incidence.

Ⅲ. Results and discussion

When the as-deposited precursor films were annealed in ambient air, V_2O_5 films with orthorhombic structure were produced in the 300 – 800 °C annealing temperature range as exhibited by the XRD spectra in Fig. 1. The spin-coated precursor films showed amorphous phase with no observable XRD peak. The V_2O_5 films obtained at and above 500 °C are seen to be fairly oriented with the crystallographic c-axis of the orthorhombic structure perpen-dicular to the substrate surface and have lattice constants close to the bulk values. On the other hand, when the as-deposited films were annealed in vacuum with the base pressure of 1×10^{-6} Torr, V_2O_3 films with rhombohedral structure were produced as exhibited by the XRD spectra in Fig. 2. It is also seen that $V_{2-x}Fe_xO_3$ (x = 0.25) films

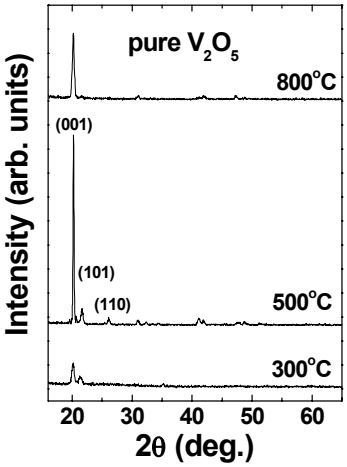

Fig. 1. XRD spectra of orthorhombic V_2O_5 films sol-gel prepared and annealed in air at different temperatures.

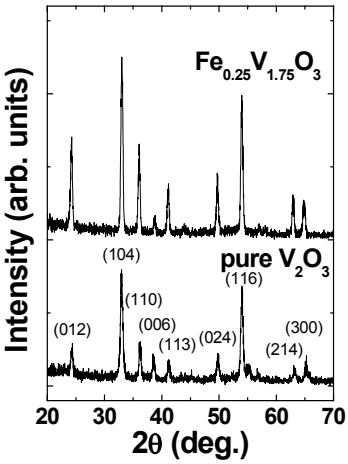

Fig. 2. XRD spectra of rhombohedral V_2O_3 and $V_{2-x}Fe_xO_3$ (x = 0.25) films.

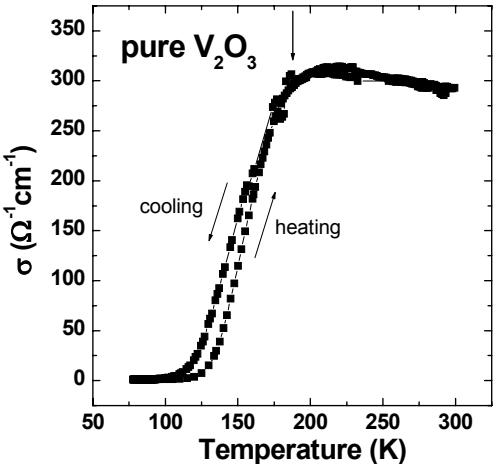

Fig. 3. Temperature dependence of electrical conductivity of rhombohedral V_2O_3 film.

prepared under the same annealing condition maintain the rhombohedral structure with little change of lattice constants. Closeness of substituting Fe^{3+} ionic radius (0.785 Å) to that of V^{3+} (0.780 Å) is attributable to the result [4]. As shown in Fig. 3, the V_2O_3 film exhibits a MI transition near 190 K (marked by an arrow), a higher temperature than that reported for a bulk. It is attributable to finite grain size of the film. Also, a hysteresis behavior is observed between cooling and heating with conductivity of 160 (cooling) and 110 $\Omega^{-1}\cdot cm^{-1}$ (heating) at 150 K.

In order to obtain VO_2 films, O_2 gas was supplied during the vacuum-annealing process. Due to the temperature-sensitiveness of the crystal structure of VO_2, the vacuum-annealed films used to contain both monoclinic (semiconducting) and tetragonal (metallic) structures. Figure 4 exhibits the variation of the XRD spectrum of the VO_2 films near 28° for different annealing condition. Pure monoclinic phase is obtained at particular O_2-gas partial pressure (10 mTorr) and annealing temperature (650 °C). Films with pure tetragonal phase were not obtained.

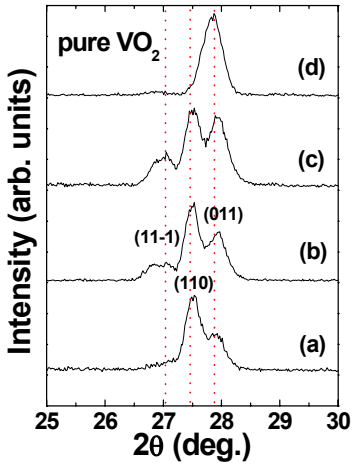

Fig. 4. XRD spectra of VO_2 films obtained by vacuum annealing under different condition: 600 °C, 2 hr (a) 800 °C, 2 hr (b) 600 °C, 2 hr with O_2 supply (10 mTorr) (c) 650 °C, 10 hr with O_2 supply (10 mTorr) (d). The (011) and (11-1) peaks are from monoclinic phase and the (110) peak is from tetragonal phase.

Hall measurements on the V_2O_5 and VO_2 films at room temperature revealed that they have n-type semiconducting properties with carrier concentration (resistivity) of about 9×10^{15} cm^{-3} (3×10^{2} $\Omega\cdot cm$) and 1×10^{16} cm^{-3} (3×10^{1} $\Omega\cdot cm$), respectively. The carrier mobility of the VO_2 films is estimated to be around 20 cm^2/Volt·sec, larger than that of

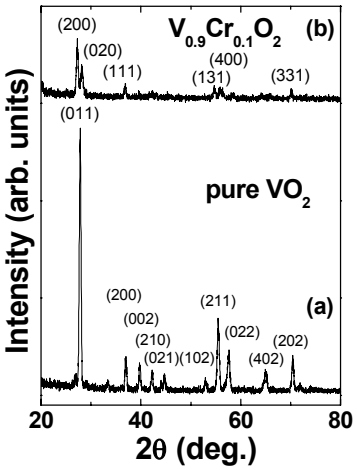

Fig. 5. Comparison of XRD spectra of pure VO_2 film with monoclinic structure (a) and $V_{1-x}Cr_xO_2$ (x = 0.1) with orthorhombic structure (b).

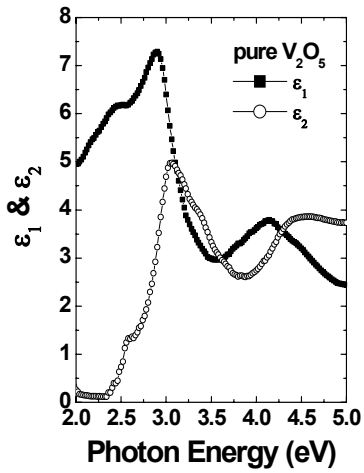

Fig. 6. Real and imaginary part of the dielectric function of orthorhombic V_2O_5 film measured by SE.

the V_2O_5 films by a factor of 10. On the other hand, the V_2O_3 films exhibit semi-metallic properties at room temperature with resistivity of about 3×10^{-3} Ω · cm. When Cr was doped into VO_2, a change in the electrical properties was observed. VO_2 film samples doped by 2 at.% Cr showed p-type character with enhanced (reduced) carrier concentration (resistivity) of 1×10^{20} cm^{-3} (2 Ω · cm) compared to that of pure VO_2. The V ion in VO_2 has a nominal valence of +4. Thus, the exhibited p-type conductivity of the VO_2:Cr film indicates that the substituting Cr ions for the octahedral V sites have a valence of +3. Due to the structural instability of VO_2 the crystal structure of the Cr-doped films ($V_{1-x}Cr_xO_2$) exhibits a phase transition to orthorhombic structure for x = 0.1 as shown in Fig. 5.

Figure 6 shows the real (ε_1) and imaginary (ε_2) parts of the dielectric function of an orthorhombic V_2O_5 film (annealed at 500 °C) measured by SE. It is seen that the optical absorption starts at about 2.3 eV, considered to be the band-gap energy of V_2O_5 [5]. The band-gap absorption of V_2O_5 has been interpreted as due to the conduction-band edge originated from the empty V 3*d* state and the valence-band edge consisting of O *2p* states.

According to the result of a band-structure calculation for orthorhombic V_2O_5, *d* bands are empty with the e_g bands being located at higher energies than the t_{2g} bands due to octahedral configuration of V ions. Also, a portion of them with $t_{2g}(d_{xy}, d_{yz})$ character equivalent to one electron state is located at lower energies compared to the rest of the *d* bands by about 0.6 eV [6]. The observed band-gap absorption is interpreted as due to the transition from the valence-band edge with O *2p* character to such $t_{2g}(d_{xy}, d_{yz})$ bands. Also, the exciton-like absorption peak at about 3 eV is interpreted as due to the transition to the main high-density $d(t_{2g})$ band edge from the O *2p* bands. The broad absorption structure at about 4.5 eV can be explained in terms of the transition to the $d(e_g)$ bands from the O *2p* bands. From the present optical data the energy difference between the center of the e_g and the t_{2g} bands, i.e., the crystal-field (CF) splitting of the octahedral V^{5+} ion in orthorhombic V_2O_5, is estimated to be about 1.5 eV.

Figure 7 exhibits the real and imaginary

part of the dielectric function of a monoclinic VO_2 film. In semiconducting VO_2 optical absorption exists at low energies below 2 eV while no absorption exists for V_2O_5 in the same energy range. Also, strong absorption structures are observed at about 2 and 3 eV. For VO_2 a part of the *d* band is filled and a Mott-Hubbard-type band gap is expected to open up between the filled and the empty $d(t_{2g})$ bands with a size of about 0.6 eV for the monoclinic structure [7]. Thus, VO_2 is expected to exhibit finite optical absorption strength above 0.7 eV while V_2O_5 does not. The 2- and 3-eV absorption peaks are interpreted as due to the $2p \rightarrow d(t_{2g})$ and $2p \rightarrow d(e_g)$, respectively. Thus, the energy difference between the center of the e_g and t_{2g} bands, i.e., the CF splitting of the octahedral V^{4+} ion in monoclinic VO_2, is estimated to be about 1.0 eV, being reduced compared to that of the orthorhombic V_2O_5. A simplified electronic band structure diagram for V_2O_5 and VO_2 containing optical transitions and CF splittings is exhibited in Fig. 8.

Figure 9 exhibits the real and imaginary part of the dielectric function of a rhombohedral V_2O_3 film. The dielectric function of V_2O_3 shows strong absorption structures at low energies, interpreted as due to its semi-metallic nature at room temperature. The smaller magnitude of the real part of the dielectric function of V_2O_3 than those of VO_2 and V_2O_5 at low energies also reflects the metallic properties of V_2O_3 at room temperature.

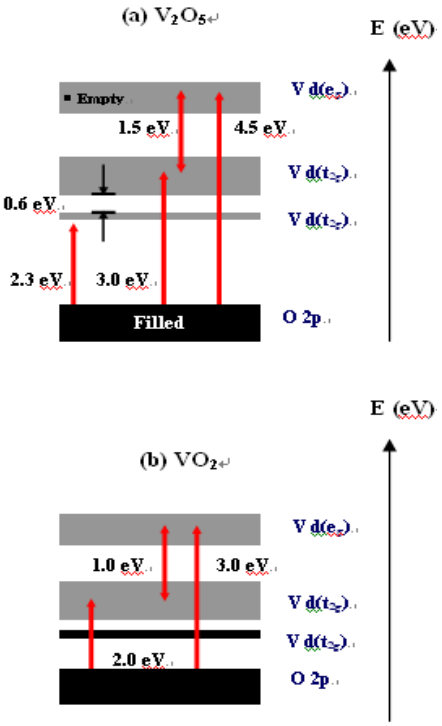

Fig. 8. Simplified electronic energy-band structure diagram for V_2O_5 (a) and VO_2 (b).

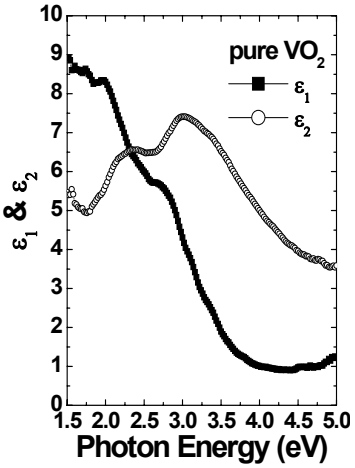

Fig. 7. Real and imaginary part of the dielectric function of monoclinic VO_2 film measured by SE.

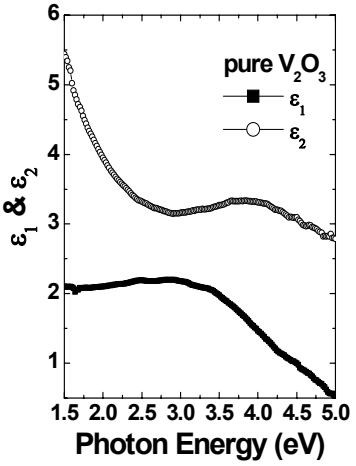

Fig. 9. Real and imaginary part of the dielectric function of rhombohedral V_2O_3 film measured by SE.

Ⅳ. Conclusion

Orthorhombic V_2O_5, monoclinic VO_2, and rhombohedral V_2O_3 thin films have been prepared by sol-gel method from single precursor solution. Annealing temperature and O_2-gas partial pressure during the post-annealing process were found to determine the crystal structure of the resultant films. The V_2O_5 and VO_2 films exhibited n-type semiconducting properties while the V_2O_3 films metallic properties investigated by Hall and SE measurements. Cr doping in VO_2 resulted in a change of conductivity type from n to p as well as a phase transformation from monoclinic to orthorhombic structure. The dielectric functions of the V_2O_5 and VO_2 films measured by SE revealed that the CF splitting between the e_g and the t_{2g} bands is about 1.5 and 1.0 eV, respectively.

Acknowledgment

This work was supported by the financial support of Konkuk University made in the program year of 2005.

References

[1] D. B. McWhan and J. P. Remeika, Phys. Rev. B 2, 3734 (1970).
[2] F. J. Morin, Phys. Rev. Lett. 3, 34 (1959).
[3] H.-T. Kim, B.-G. Chae, D.-H. Youn, S.-L. Maeng, G. Kim, K.-Y. Kang, and Y.-S. Lim, New J. Phys. 6, 52 (2004).
[4] R. D. Shannon, Acta Crystallogr., Sect. A 32, 751 (1976).
[5] M. Losurdo, G. Bruno, D. Barreca, and E. Tondello, Appl. Phys. Lett. 77, 1129 (2000).
[6] J. C. Parker, D. J. Lam, Y.-N. Xu, and W. Y. Ching, Phys. Rev. B 42, 5289 (1990).
[7] A. Bianconi, S. Stizza, and R. Bernardini, Phys. Rev. B 24, 4406 (1981).

≪연구논문≫한국진공학회지 제15권 5호, 2006년 9월, pp.534~540

바나듐 옥사이드 박막의 성장 및 그 구조적, 전기적, 광학적 특성

박영란 · 김광주*

건국대학교 물리학과, 서울시 광진구 화양동 1번지, 143-701

(2006년 7월 10일 받음)

V_2O_3, VO_2, V_2O_5 박막들이 하나의 선구 용액으로부터 다양한 후열처리 조건을 통하여 제작될 수 있었다. 진공 중 후열처리 시 rhombohedral 구조의 V_2O_3 박막이 형성되어졌고, 공기 중 후열처리 시 orthorhombic 구조의 V_2O_5 박막을 얻을 수 있었다. Monoclinic 구조의 VO_2 박막은 진공 후열처리 중 O_2 가스를 공급함으로써 제작될 수 있었다. V_2O_3 박막이 상온에서 도체적 특성을 보이는 반면, V_2O_5, VO_2 박막은 반도체적 성질을 지니고 있음을 전기적, 광학적 특성 조사를 통하여 알 수 있었다. 크롬(Cr)이 도핑됨에 따라 VO_2 박막은 그 전기전도성이 n-type에서 p-type으로 변화하였고 비저항이 감소되는 결과를 나타내었다. 또한, 크롬 도핑된 VO_2 박막은 orthorhombic 구조를 나타내었다. 이와 같은 바나듐 옥사이드 박막들에서 관측된 광학적 흡수 구조들은 O *2p* 에서 V *3d* 밴드로의 전이에 의한 것으로 해석되어진다. 바나듐 이온의 t_{2g} 상태와 e_g 상태 사이의 결정장 갈라짐(crystal-field splitting)은 V_2O_5와 VO_2에 대해서 각각 1.5 및 1.0 eV로 해석된다.

주제어 : 바나듐 옥사이드; 졸-겔 방법; 구조적 특성; 광학적 특성

* [전자우편] kjkim@konkuk.ac.kr